© SEP 2025 | IRE Journals | Volume 9 Issue 3 | ISSN: 2456-8880
DOI: https://doi.org/10.64388/IREV9I3-1722729

Structural, Optical, and Bandgap Engineering of Co-Precipitated Ni-Doped ZnO Nanoparticles

AKANKSHA CHANDRAKANT JAWLE
Department of Physics, Kai. Rasika Mahavidyalaya, Deoni, Dist. Latur, Maharashtra, INDIA

Abstract- ***Ni-doped zinc oxide (ZnO) particles were prepared using the co-precipitation method. We studied the changes in structural and optical properties of ZnO nanoparticles at different doping concentration of Ni. X-ray diffraction (XRD) patterns confirm the wurtzite crystal structure of ZnO and polycrystalline nature. Also, XRD date revealed that with an increase in Ni doping level, there is decrease in lattice parameters. The crystallite size decreases with increase in Ni doping concentration confirmed a successfully incorporation of Ni in the ZnO host matrix. The optical property is investigated by UV-Vis spectroscopy and found that the optical band gap values decreased from 3.39 to 3.26 eV after Ni doping because of p-d exchange interaction.***

Keywords: Ni-doped ZnO; co-precipitation; crystallite size; UV-Vis spectroscopy; optical band gap.

I. INTRODUCTION

In the past decades, transition metal oxide (TMO) based semiconductors have attracted immense interest due to their potential applications in spintronics, gas sensors, LEDs, optoelectronics, and energy storage devices [1 - 4]. As an important property of TMO, semiconductor material with a broad simple bandgap is under extensive study so that it is use in optoelectronics device applications [5, 6]. Recently, considerable interests have focused on the magnetic and optical properties of TMO because of inexpensive and nontoxic material that can be easily produced with high chemical and mechanical stability [7]. Compared with their other TMO, zinc oxide (ZnO) is promising materials for spintronics and optoelectronics devices due to its excellent semiconducting property and broad band gap (3.33eV) [8]. Due to its superior optoelectronic profile most notably high optical transmittance across the visible and near-infrared spectra zinc oxide (ZnO) is widely recognized as a pivotal metal oxide [9]. Beyond its tailored bandgap properties, ZnO offers distinct practical advantages such as low cost, environmental benignity, and high chemical and mechanical durability. These features make it an attractive platform for integration into photo-voltaics, advanced optoelectronics, and heterogenous catalysis [10 - 13].

Transition metal (TM)-doped zinc oxide (ZnO) has emerged as a compelling material system, combining charge and spin degrees of freedom for UV sensors and spintronic devices [14, 15]. Incorporating TM dopants modulates the optical, electrical, and mechanical properties of ZnO via quantum confinement effects. Consequently, extensive research has focused on tailoring ZnO nanostructures across various dimensionalities including 1D (nanowires, nanotubes, nanopipes), 2D (nanoplatelets), and 3D (nanoparticles) morphologies to optimize performance for advanced functional applications [16].

Tuning the bandgap and transport properties of ZnO via dopant engineering is critical for optimizing photo-detector performance without compromising sensitivity. In particular, Ni^{2+} substitution is exceptionally viable allowing seamless lattice integration within the wurtzite matrix. Incorporating transition metal ions like Ni^{2+} enhances charge carrier generation and transport, yielding superior UV photoresponse, thermal stability, and optoelectronic performance compared to pristine ZnO [17].

Herein we report the co-precipitation synthesis, characterization and optoelectronics applications of new Zinc Oxide based nanoparticles i.e. nanoparticles. All this nanoparticles of undoped and ni-doped were characterized for their crystal structure, crystallite size, lattice parameters were investigated. Finally the optical properties of zinc oxide nanoparticles of different doping of nickel are reported.

© SEP 2025 | IRE Journals | Volume 9 Issue 3 | ISSN: 2456-8880
DOI: https://doi.org/10.64388/IREV9I3-1722729

II. EXPERIMENTATION

Undoped and Ni-doped ZnO nanoparticles were synthesized via a co-precipitation route. For pure ZnO (x = 0.00), stoichiometric amounts of high-purity zinc acetate dihydrate and potassium hydroxide KOH were separately dissolved in 50 mL of double-distilled water. The KOH solution was added drop wise to the zinc precursor solution under continuous magnetic stirring for 2h.

For the Ni-doped samples (x = 0.02, 0.04 and 0.06), required molar ratios of zinc acetate dihydrate and nickel acetate tetrahydrate were dissolved together in 50 mL of double-distilled water, while KOH was dissolved in 50 mL of methanol. The alkaline solution was subsequently introduced into the precursor mixture under vigorous magnetic stirring for 2h.The resulting precipitates were collected via filtration, washed thoroughly with double-distilled water to remove residual impurities, and dried at 150 ^{0}C. Finally, the dried powders were annealed at 400 ^{0}C for 4h to obtain crystalline Ni-doped ZnO nanoparticles. Structural properties were studied using X-ray diffractometer (Model: PW-3710). Optical properties investigated using UV-Vis spectrophotometer (JASCO-7310) in the wavelength range of 200–800 nm with a step size of 2nm.

III. RESULTS AND DISCUSSION

A) Structural study

The phase purity of the ZnO nanoparticles of different doping levels of Ni was investigated based on the XRD patterns as shown in fig. 1. All the observed diffraction peaks were in worthy arrangement with the hexagonal ZnO as per the 80-0075 JCPDS data file card. Also, no evidence for extra impurity phases was detected in the XRD pattern. The peaks indexed to the (100), (002), (101), (102), (110), (103) and (112) planes in the XRD patterns were sharp which proposes a polycrystalline nature of the prepared undoped and Ni-doped ZnO particles.

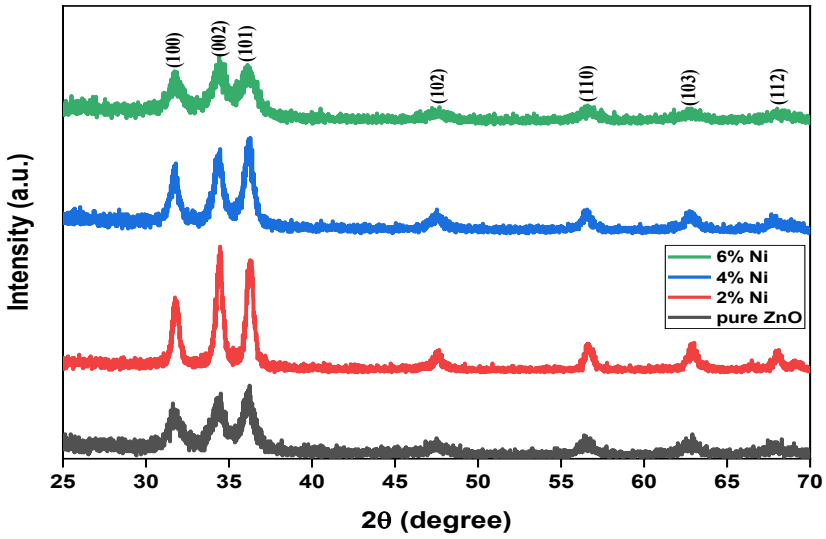

Fig.1. XRD patterns of undoped and Ni-doped ZnO nanoparticles.

As Ni doping increase, the most intense peaks of (100), (002) and (101) are shifted to the higher angle as shown in fig. 2. This could be ascribed to the difference between the radii of Ni^{2+} and Zn^{2+}. From fig. 2, it is also clear that the intensity of these peaks decreases gradually after Ni doping indicating the incorporation of Ni^{2+} ions into the ZnO host matrix [18]. The average crystallite sizes of undoped and Ni-doped ZnO nanoparticles are estimated from full width at half maximum of XRD peaks by Scherrer's formula [19]. The average crystallite size and dislocation density of prepared nanoparticles are given in table 1.

© SEP 2025 | IRE Journals | Volume 9 Issue 3 | ISSN: 2456-8880
DOI: https://doi.org/10.64388/IREV9I3-1722729

The average crystallite sizes of pure, 2% Ni, 4%Ni and 6% Ni-doped ZnO nanoparticles are found to be 20.73 nm, 19.04 nm, 14.66 nm, and 9.91 nm respectively. The dislocation density of ZnO is found to be increase from 2.327×10^{-3} nm^{-2} to 10.73×10^{-3} nm^{-2}estimated from crystallite size.

The incorporation of Ni^{2+} ions can also be verified by the change in lattice parameters and cell volume as function of Ni doping. The lattice parameters "a" and "c" are found to decrease with an increase in Ni content as shown in table 1. The cell volume of ZnO is higher as compared to the Ni-doped ZnO nanoparticles due to the smaller ionic radii of Ni^{2+} as compared to Zn^{2+} ions [20].

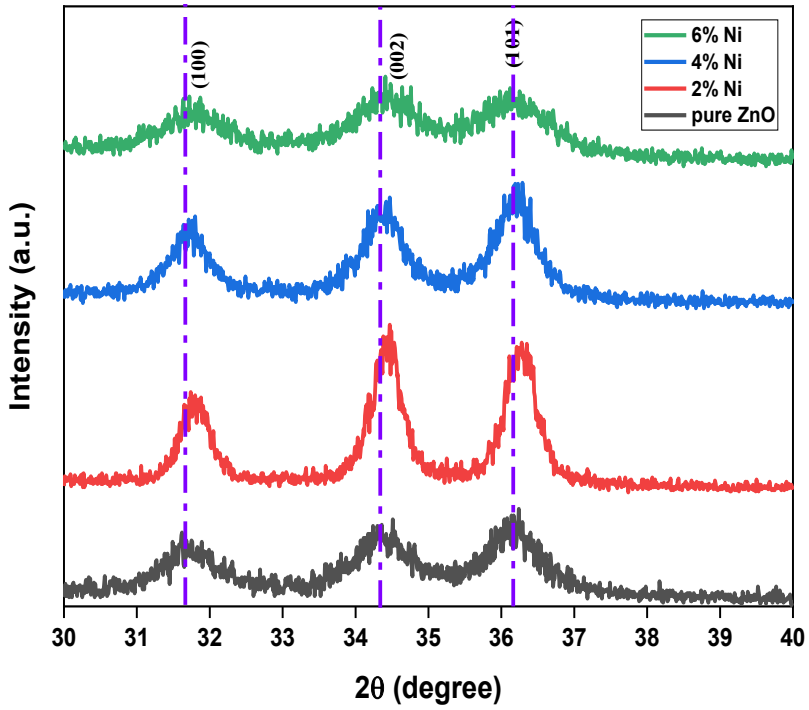

Fig.2. Diffraction peaks of (100), (002) and (101) broadening of undoped and Ni-doped ZnO nanoparticles.

Table 1. Structural parameters of undoped and Ni-doped ZnO nanoparticles.

Structural Parameters	ZnO	2% Ni	4% Ni	6% Ni
a (Å)	3.2539	3.2499	3.2495	3.2427
c (Å)	5.2098	5.2066	5.2069	5.1948
Volume of cell $(Å)^3$	47.77	47.62	47.61	47.31
D (nm)	20.73	19.04	14.66	9.91
Dislocation density (nm^{-2})	2.327×10^{-3}	2.758×10^{-3}	4.649×10^{-3}	10.173×10^{-3}

B) Optical studies

The optical absorption of undoped and Ni-doped ZnO nanoparticles is represents in fig. 3. All nanoparticles are measured between 200 nm to 800 nm. All prepared films are positioned in the visible region and the variation of absorption edge is found to be 300 nm to 350 nm. The absorption edge is going to increase with increase in Ni-doping. It may be due to decrease in crystallite size and surface roughness [21].

© SEP 2025 | IRE Journals | Volume 9 Issue 3 | ISSN: 2456-8880
DOI: https://doi.org/10.64388/IREV9I3-1722729

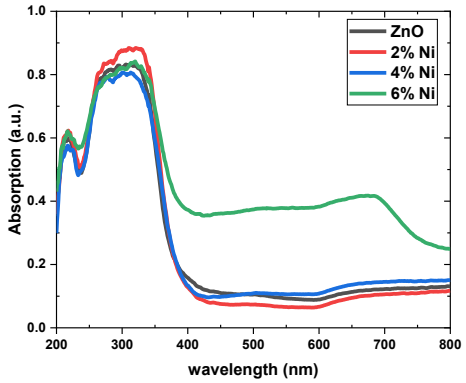

Fig.3. Optical absorption spectra of undoped and Ni-doped ZnO nanoparticles.

The optical band gap results of the prepared nanoparticles were calculated via the principal of absorption energy which associated with electron excitation from valence band to the conduction band. Absorption coefficient and photon energy are two factors plays an important role in determining band gap energy given by relations [22]

$$\alpha h\nu = A(h\nu - E_g)^2 \quad (1)$$

Where, A is a constant and E_g is the optical gap. Fig. 4 showed that the square of the optical absorption coefficient versus photon energy (Tauc plot). Tauc's plot technique was used to determine the optical direct band gap of undoped and Ni-doped ZnO nanoparticles. The optical band gap decreased with increase in Ni concentration. 3.39 eV for undoped ZnO and 3.38 eV, 3.34 eV, 3.26 eV respectively for 2%, 4%, 6% Ni-doped ZnO nanoparticles. The band gap decrease after incorporation of Ni because of sp-d exchange interaction between the the band electrons and the localized d electrons of Ni^{2+} ions. Similar results were obtained by previous reported literature [23].

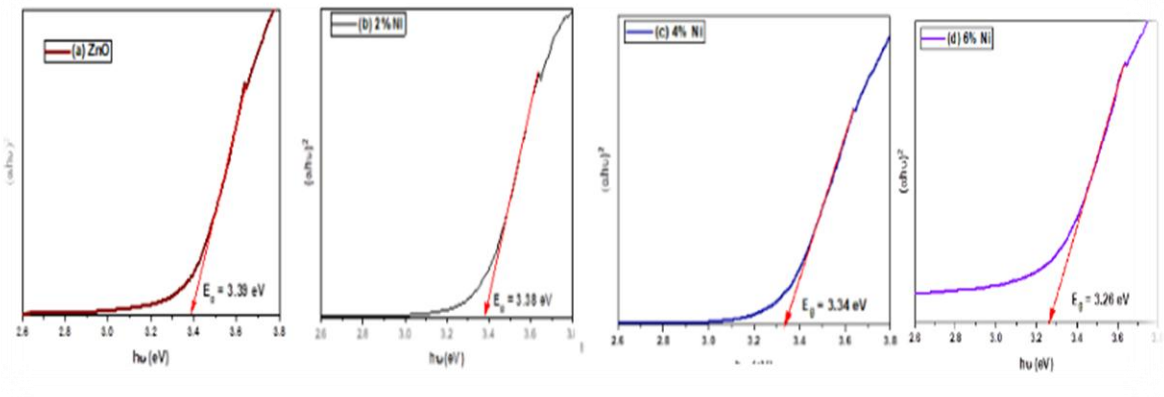

Fig.4. Optical band gap values of undoped and Ni-doped ZnO nanoparticls.

IV. CONCLUSION

Undoped ZnO and Ni-doped ZnO nanoparticles at different doping concentration of Ni was successfully synthesized via co-precipitation method. XRD patterns revealed that all synthesized samples have wurtzite (hexagonal) crystal structure of ZnO. The lattice parameters and cell volume of ZnO was decreased with increase in Ni doping. The average crystallite size was going to be decrease from 20.73 nm to 9.91 nm. The dislocation density was increases after Ni-doping indicating that Ni ions successfully incorporation in the ZnO host lattice. The absorption edge decrease with increase in Ni doping and the optical band gap decreased from 3.39 eV to 3.26 eV. Therefore, Ni-doped ZnO samples have a potential to become a satisfactory optoelectronics material in future.

REFERENCES

[1] Xu, F., & Ho, H.-P. (2017). Light-Activated Metal Oxide Gas Sensors: A Review.

Micromachines, 8(11), 333. https://doi.org/10.3390/mi8110333.

[2] Yang, S., Lei, G., Xu, H., Lan, Z., Wang, Z., & Gu, H. (2021). Metal Oxide Based Heterojunctions for Gas Sensors: A Review. Nanomaterials, 11(4), 1026. https://doi.org/10.3390/nano11041026.

[3] S. George, N., Maria Jose, L., & Aravind, A. (2023). Review on Transition Metal Oxides and Their Composites for Energy Storage Application. Updates on Supercapacitors. https://doi.org/10.5772/intechopen.108781.

[4] Han, Y., Lao, B., Zheng, X., Li, S., Li, R.-W., & Wang, Z. (2024). Transition metal oxides: a new frontier in spintronics driven by novel quantum states and efficient charge-spin interconversion. Frontiers in Materials, 11. https://doi.org/10.3389/fmats.2024.1444769.

[5] Park, S., et al. (2019). Exploring wide bandgap metal oxides for perovskite solar cells. AIP Advances, 9(2), 022401.DOI: 10.1063/1.5081822.

[6] Pearton, S. J., et al. (2010). Review of wide bandgap semiconductor materials and devices. Journal of Vacuum Science & Technology B, 28(3), 407–438. DOI: 10.1116/1.3368581.

[7] Ashour, M., Mansour, A. T., Abdelwahab, A. M., & Alprol, A. E. (2023). Metal Oxide Nanoparticles' Green Synthesis by Plants: Prospects in Phyto- and Bioremediation and Photocatalytic Degradation of Organic Pollutants. Processes, 11(12), 3356. https://doi.org/10.3390/pr11123356.

[8] Di Trolio, A., Testa, A. M., & Amore Bonapasta, A. (2022). Ferromagnetic Behavior and Magneto-Optical Properties of Semiconducting Co-Doped ZnO. Nanomaterials, 12(9), 1525. https://doi.org/10.3390/nano12091525.

[9] Arifin, N. M., Mhd Noor, E. E., Mohamad, F., & Mohamad, N. (2024). The Impact of Spinning Speed on n-TiO2/ZnO Bilayer Thin Film Fabricated through Sol–Gel Spin-Coating Method. Coatings, 14(1), 73. https://doi.org/10.3390/coatings14010073.

[10] Arifin, N. M., Mhd Noor, E. E., Mohamad, F., & Mohamad, N. (2024). The Impact of Spinning Speed on n-TiO_2/ZnO Bilayer Thin Film Fabricated through Sol–Gel Spin-Coating Method. Coatings, 14(1), 73. https://doi.org/10.3390/coatings14010073.

[11] Calnan, S. (2014). Applications of Oxide Coatings in Photovoltaic Devices. Coatings, 4(1), 162–202. https://doi.org/10.3390/coatings4010162.

[12] Sahoo, S., Wickramathilaka, K. Y., Njeri, E., Silva, D., & Suib, S. L. (2024). A review on transition metal oxides in catalysis. Frontiers in Chemistry, 12, 1374878. https://doi.org/10.3390/fchem.2024.1374878.

[13] Wang, X., Ahmad, M., & Sun, H. (2017). Three Dimensional ZnO Hierarchical Nanostructures: Solution Phase Synthesis and Applications. Materials, 10(11), 1304. https://doi.org/10.20944/preprints201710.0121.v1.

[14] Pearton, S. J., Norton, D. P., Ivill, M. P., Hebard, A. F., Zavada, J. M., Chen, W. M., & Buyanova, I. A. (2007). ZnO Doped With Transition Metal Ions. IEEE Transactions on Electron Devices, 54(5), 1040–1048. DOI: 10.1109/TED.2007.894371

[15] Dietl, T. (2010). A ten-year perspective on dilute magnetic semiconductors and oxides. Nature Materials, 9(12), 965–974. DOI: 10.1038/nmat2898.

[16] Thejas, S., et al. (2025). A Review on ZnO Nanostructures for Biosensors and Functional Applications. Journal of Electronic Materials, 54(2), 1120–1138. DOI: 10.1007/s11664-024-11580-2.

[17] Vijayalakshmi, R., et al. (2013). Influence of Ni doping on the structural, optical, and photoresponse properties of ZnO thin films. Journal of Materials Science: Materials in Electronics, 24(10), 3805–3810. DOI: 10.1007/s10854-013-1321-y

[18] Tang, L., Jia, Y., Zhu, Z., Hua, Y., Wu, J., Zou, Z., & Zhou, Y. (2022). Effects of Co Doping on the Growth and Photocatalytic Properties of ZnO Particles. Molecules, 27(3), 833. https://doi.org/10.3390/molecules27030833.

[19] Patterson, A. L. (1939). The Scherrer Formula for X-Ray Particle Size Determination. Physical

Review, 56(10), 978–982. DOI: 10.1103/PhysRev.56.978.

[20] Ali, M. Y., Khan, M. K. R., Karim, A. M. M. T., Rahman, M. M., & Kamruzzaman, M. (2020). Effect of Ni doping on structure, morphology and opto-transport properties of spray pyrolised ZnO nano-fiber. Heliyon, 6(3), e03588. https://doi.org/10.1016/j.heliyon.2020.e03588.

[21] Toma, M., Selyshchev, O., Havryliuk, Y., Pop, A., & Zahn, D. R. T. (2022). Optical and Structural Characteristics of Rare Earth-Doped ZnO Nanocrystals Prepared in Colloidal Solution. Photochem, 2(3), 515–527. https://doi.org/10.3390/photochem2030036.

[22] Tauc, J., Grigorovici, R., & Vancu, A. (1966). Optical Properties and Electronic Structure of Amorphous Germanium. Phys. Stat. Sol. (b), 15(2), 627–637. DOI: 10.1002/pssb.19660150224.

[23] Srinivasan, R., et al. (2017). Structural, optical, and magnetic properties of Ni-doped ZnO nanoparticles synthesized by co-precipitation method. Journal of Materials Science: Materials in Electronics, 28(21), 16223–16231.